Implications of the Higgs discovery in the MSSM golden region

Ian Low and Shashank Shalgar

Theory Group, HEP Division, Argonne National Laboratory,
Argonne, IL 60439, U.S.A.
Department of Physics and Astronomy, Northwestern University,
Evanston IL 60208, U.S.A.

E-mail: ilow@northwestern.edu, shashankshalgar@u.northwestern.edu

ABSTRACT: If the lightest CP-even Higgs boson in the MSSM is discovered at the LHC, two measurements could be made simultaneously: the Higgs mass m_h and the event rate $B\sigma(gg \to h \to \gamma\gamma)$. We study to what extent the combination of these two measurements would allow us to extract parameters in the stop mass matrix, including the off-diagonal mixing term, with a focus on the MSSM golden region where the stops are light and the mixing is large. Even though both the production cross-section and the decay amplitude are not sensitive to supersymmetric parameters outside of the stop sector, the branching ratio depends on the total decay width, which is dominated by the Higgs decay to b quarks and sensitive to both the pseudo-scalar mass m_A and the supersymmetric Higgs mass μ. In the end we find m_A is an important input in extracting the stop mass parameters, while a fair estimate of the off-diagonal mixing term could be obtained without prior knowledge of μ.

JHEP04(2009)091

Contents

1 Introduction

Supersymmetry (SUSY) is widely considered as the leading proposal to address the hierarchy problem in the standard model. The simplest realization of SUSY, the mininal supersymmetric standard model (MSSM), is without a doubt the most popular extension of the standard model in the last three decades. Although a theoretically very appealing concept, SUSY has remained elusive in experimental searches despite tremendous amount of efforts. The non-discovery of any new particles or the Higgs boson to date introduces a certain amount of fine-tuning in the electroweak sector of MSSM [1, 2] and creates a somewhat awkward situation given SUSY's promise to solve the electroweak hierarchy problem.

There is, however, a particular region in the parameter space of MSSM where the fine-tuning in the Higgs mass is reduced. It is the region where the overall stop mass scale is light at several hundreds GeV and the mixing in the stop sector is maximized due to a large trilinear soft A_t term, which implies two stop mass eigenstates below 1 TeV with a mass splitting in the order of a few hundreds GeV. Such a region is dubbed the "golden region" of MSSM by Perelstein and Spethmann in ref. [3] because it satisfies the experimental constraints, including the bound of 114 GeV on the Higgs mass, and minimizes the unnaturalness in the MSSM. Obviously implications of the MSSM golden region on the possible collider signatures at the Large Hadron Collider (LHC) deserve detailed studies if one wish to take the naturalness argument seriously. Previous works on the phenomenology of MSSM golden region can be found in refs. [3–9].

In this work we wish to study the implication of discovering the lightest CP-even Higgs in the MSSM golden region. Since the Higgs sector of the MSSM contains two Higgs doublets, after electroweak symmetry breaking there are five scalar Higgs bosons remaining: a pair of charged Higgs $H^{\pm}$, one CP-odd Higgs A, two CP-even Higgses h and H where H is defined to be the heavier one. Moreover, it is found that, after including radiative corrections, there is an upper bound on the mass of the lightest CP-even Higgs at roughly $130 - 140$ GeV. (For a recent review, see ref. [10].) The importance of such a bound lies in

the observation that a Higgs boson in this mass range can be discovered at the LHC only through its decay into $\gamma\gamma$, which is a loop-induced process, because its mass is below the W^+W^- and ZZ thresholds; decays into $b\bar{b}$ pair are swamped by the background. On the other hand, the dominant production mechanism of the neutral Higgs boson at the LHC is the gluon fusion process [11], also a loop induced process. Since both production and decay channels are loop induced, and hence very sensitive to effects of new physics if any, the process $gg \to h \to \gamma\gamma$ is the natural playground to look for deviations from standard model predictions.

Within MSSM effects of supersymmetric particles in the production cross-section $\sigma(gg \to h)$ and the partial decay width $\Gamma(h \to \gamma\gamma)$ have been studied previously [12, 13]. It is found that for both amplitudes the leading corrections come from the stop sector and, to a lesser extent, charged SUSY particles such as the charginos. However, it is important to emphasize that, once the Higgs is discovered in the process $gg \to h \to \gamma\gamma$, two experimental measurements can be made at the same time: the event rate $\sigma(gg \to h) \times Br(h \to \gamma\gamma)$ and the Higgs mass m_h. One should therefore make use of the information from both measurements in trying to extract parameters of the MSSM. Indeed, ref. [5] showed that it is possible to obtain a fairly good estimate on the trilinear soft A_t term in the stop sector, which is otherwise difficult to measure, if one combines knowledge on the production cross section in the gluon fusion channel $\sigma(gg \to h)$ and m_h. One limitation of the proposal in [5] is that the production cross section $\sigma(gg \to h)$ is not directly observable in collider experiments:[1] only the product $\sigma(gg \to h) \times Br(h \to \gamma\gamma)$ is. Therefore, in this note we will study implications of combining two measurements, $\sigma \times Br$ and m_h, in $gg \to h \to \gamma\gamma$ with an emphasis on the golden region of the MSSM parameter space.

2   Higgs couplings to gg and $\gamma\gamma$ in the MSSM

In this section we discuss the effects of superparticles on the Higgs coupling to two gluons and two photons. In particular, we will work in the so-called decoupling limit [16] where the pseudo-scalar Higgs is much heavier than the Z boson: $m_A \gg m_Z$. There are two reasons for considering the decoupling limit. The first is the lightest CP-even Higgs quickly reaches its maximal possible mass, which is phenomenologically desirable given the null result for Higgs searches at both LEP and Tevatron. The second reason is the tree-level couplings of h in the MSSM to standard model fermions and gauge bosons approach the values for a standard model Higgs, and the two become almost indistinguishable. Therefore any deviations in the event rate from the standard model would come from effects of superparticles running in the loop. It is also worth mentioning that in this case all other Higgs bosons in the MSSM are roughly degenerate $m_A \approx m_H \approx m_{H^\pm}$. In practice, the decoupling limit is quickly reached for moderately large m_A gets larger than the maximal possible value for h:the decoupling limit is reached when $m_A \gtrsim 300\,\mathrm{GeV}$. However, we will see later that Higgs couplings to vector bosons approach the decoupling limit much faster than Higgs couplings to fermions, which has important implications in the present study.

---

[1]There are, nevertheless, ways to extract this cross section at the LHC with an uncertainty in the order of $30 - 40\%$ [14], even though a recent study suggests a smaller uncertainty may be possible [15].

Analytic expressions for a CP-even scalar Higgs decaying into two gluons and two photons within the standard model were obtained long ago in refs. [17–19]. The loop induced amplitude $h \to gg$ is mediated by the top quark, which has the largest coupling to the Higgs among the fermions, whereas $h \to \gamma\gamma$ has the leading contribution from the W boson loop with the top quark as the subleading contribution. In the MSSM expressions for effects of superpartners can be found in ref. [20]. In $h \to gg$ the top squark gives the dominant supersymmetric contribution, while all the charged superparticles, such as the sfermions, charged Higgs scalars, and the charginos, now contribute to $h \to \gamma\gamma$ as well. More explicitly,

$$\Gamma(h \to gg) = \frac{G_F \alpha_s^2 m_h^3}{36\sqrt{2}\pi^3} \left| N_c \, Q_t^2 \, g_{htt} \, A_{\frac{1}{2}}^h(\tau_t) + \mathcal{A}^{gg} \right|^2, \tag{2.1}$$

$$\Gamma(h \to \gamma\gamma) = \frac{G_F \alpha^2 m_h^3}{128\sqrt{2}\pi} \left| N_c \, Q_t^2 \, g_{htt} \, A_{1/2}^h(\tau_t) + g_{hWW} \, A_1^h(\tau_W) + \mathcal{A}^{\gamma\gamma} \right|^2, \tag{2.2}$$

where g_{htt} and g_{hWW} are the coupling of h to the top quark and the W boson, respectively. Moreover $\tau_i = m_h^2/(4m_i^2)$ and the form factors are

$$A_{\frac{1}{2}}^h(\tau) = \frac{2}{\tau^2}[\tau + (\tau - 1)f(\tau)], \tag{2.3}$$

$$A_0^h(\tau) = -\frac{1}{\tau^2}[\tau - f(\tau)], \tag{2.4}$$

$$A_1^h(\tau) = -\frac{1}{\tau^2}[2\tau^2 + 3\tau + 3(2\tau - 1)f(\tau)], \tag{2.5}$$

$$f(\tau) = \begin{cases} \arcsin^2 \sqrt{\tau} & \tau \le 1 \\ -\frac{1}{4}\left[\log \frac{1 + \sqrt{1 - \tau^{-1}}}{1 - \sqrt{1 - \tau^{-1}}} - i\pi\right]^2 & \tau > 1 \end{cases}. \tag{2.6}$$

The supersymmetric contributions $\mathcal{A}^{gg}$ and $\mathcal{A}^{\gamma\gamma}$ are

$$\mathcal{A}^{gg} = \sum_i N_c \, Q_t^2 \, g_{h\tilde{t}_i\tilde{t}_i} \frac{m_Z^2}{m_{\tilde{t}_i}^2} A_0^h(\tau_{\tilde{t}_i}), \tag{2.7}$$

$$\mathcal{A}^{\gamma\gamma} = g_{hH^+H^-} \frac{m_W^2}{m_{H^\pm}^2} A_0^h(\tau_{H^\pm}) + \sum_f N_c Q_f^2 \, g_{hf\tilde{f}} \frac{m_Z^2}{m_{\tilde{f}}^2} A_0^h(\tau_{\tilde{f}}) + \sum_i g_{h\chi_i^+\chi_i^-} \frac{m_W}{m_{\chi_i}} A_{\frac{1}{2}}^h(\tau_{\chi_i}). \tag{2.8}$$

Explicit forms for the couplings of h to superparticles can be found in refs. [10, 20]. We will, however, write down $g_{h\tilde{t}_i\tilde{t}_i}$ since the stop contribution is the focus of present study. When normalizing to $2m_Z^2(\sqrt{2}G_F)^{1/2}$,

$$g_{h\tilde{t}_1\tilde{t}_1} = \cos 2\beta \left(\frac{1}{2}\cos^2\theta_t - \frac{2}{3}s_w^2 \cos 2\theta_t\right) + \frac{m_t^2}{m_Z^2} - \frac{1}{2}\frac{m_t X_t}{m_Z^2}\sin 2\theta_t, \tag{2.9}$$

$$g_{h\tilde{t}_2\tilde{t}_2} = \cos 2\beta \left(\frac{1}{2}\sin^2\theta_t + \frac{2}{3}s_w^2 \cos 2\theta_t\right) + \frac{m_t^2}{m_Z^2} + \frac{1}{2}\frac{m_t X_t}{m_Z^2}\sin 2\theta_t. \tag{2.10}$$

In the above s_w is the sine of Weinberg angle and θ_t is the mixing angle in the stop sector. The mixing parameter X_t is the off-diagonal entry in the stop mass matrix

$$M_{\tilde{t}}^2 = \begin{pmatrix} m_{\tilde{t}_L}^2 + m_t^2 + D_L^t & m_t X_t \\ m_t X_t & m_{\tilde{t}_R}^2 + m_t^2 + D_R^t \end{pmatrix}, \tag{2.11}$$

– 3 –

where

$$D_L^t = \left(\frac{1}{2} - \frac{2}{3}s_w^2\right) m_Z^2 \cos 2\beta, \tag{2.12}$$

$$D_R^t = \frac{2}{3}s_w^2 m_Z^2 \cos 2\beta, \tag{2.13}$$

$$X_t = A_t - \frac{\mu}{\tan\beta}. \tag{2.14}$$

In the limit of heavy loops masses $\tau_i \ll 1$, the form factors approach the asymptotic values

$$A_0^h \to -\frac{1}{3}, \quad A_{\frac{1}{2}}^h \to -\frac{4}{3}, \quad A_1^h \to +7 . \tag{2.15}$$

Note that standard model contributions due to the top quark and W boson loops are finite in the asymptotic limit, whereas the supersymmetric contributions are suppressed by large loop masses. One exception is the stop contribution in the MSSM golden region when the stops are light and the mixing parameter X_t is large. In this case the stop mixing angle is maximal, $|\sin 2\theta_t| \approx 1$, and the $g_{h\tilde{t}_i\tilde{t}_i}$ coupling is strongly enhanced. Thus the stop correction in the Higgs production and decay amplitudes is the dominant one and very pronounced, despite being a loop effect. The particle giving the second largest effect is the chargino, not only because its effect decouples like $1/m_{\tilde{\chi}}$ when others decouple like $1/m^2$, as can be seen in $\mathcal{A}^{\gamma\gamma}$, but also because of the larger asympotic value of $A_{1/2}^h$ than A_0^h.

For the gluon fusion production, it has been shown that the stop could have an order unity effect when comparing with the standard model rate, especially in the region of light stops and large mixing X_t [5, 13], which is exactly the MSSM golden region. As for the Higgs decay into two photons, ref. [12] showed that the stop could have a sizable effect, in the order of 10% level, in the MSSM golden region. The effect is less dramatic than in the gluon fusion rate because the W boson loop is the dominant contribution in the decay into two photons, as can be seen from eq. (2.15), which shows A_1^h has the largest asymptotic value. Moreover, among all the charged superparticles only the chargino loop could have a significant effect again in the order of 10% when the chargino is as light as $100\,\mathrm{GeV}$. For chargino masses above $250\,\mathrm{GeV}$, the deviation is less than 8% through out the entire MSSM parameter space [12]. The direct search limit of charginos from LEP is at $103\,\mathrm{GeV}$, which is quite robust and independent of model assumptions, whereas searches at Tevatron result in a lower bound of $145\,\mathrm{GeV}$ in a specific model choice [21]. In section IV we will demonstrate that throughout the MSSM golden region the chargino has a small effect, when considering the ratio of the event rate $\sigma(gg \to h) \times Br(h \to \gamma\gamma)$ in the MSSM over the SM, once its mass is heavier than $200\,\mathrm{GeV}$.

In addition to focusing on the region of MSSM parameter space where the stops are light and the mixing is large, we would follow ref. [5] and concentrate on the following choice of parameters:

- $10 \lesssim \tan\beta \lesssim m_t/m_b,$

- $|m_b\mu\tan\beta| \lesssim m_{\tilde{b}_L}^2,\ m_{\tilde{b}_R}^2,$
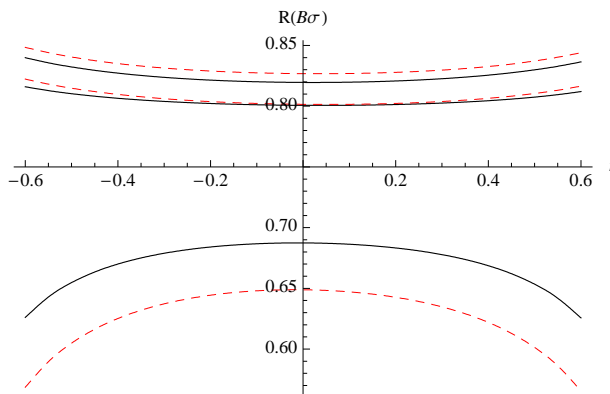
Figure 1. Plot of $R(B\sigma) = B\sigma(\text{MSSM})/B\sigma(\text{SM})$ as a function of r for $m_{\tilde{t}} = 500\,\text{GeV}$, $m_A = 400\,\text{GeV}$, $\mu = 200\,\text{GeV}$,and $M_{\text{SUSY}} = 1\,\text{TeV}$. The (dark) solid and (red) dashed lines are for $\tan\beta = 10$ and 40, respectively. The three sets of curves from top to bottom are for $X_t/m_{\tilde{t}} = 0, -1$, and -2 respectively.

The main reason for doing so is to avoid the region where the sbottom contribution could be significant in the loop induced processes [13] as well as the Higgs mass [22]. Furthermore, the mass of the lightest CP-even Higgs is insensitive to $\tan\beta$ once $\tan\beta \gtrsim 10$. Since the bottom quark mass is very small $m_b \sim 5\,\text{GeV}$, the above choice covers a very substantial region of MSSM parameter space.

Another important comment is related to the observation made in ref. [5] where it was shown that the gluon fusion production rate depends on only two out of the three parameters in the stop mass matrix in eq. (2.11). If we define the following parameters

$$m_{\tilde{t}}^2 = \frac{m_{\tilde{t}_L}^2 + m_{\tilde{t}_R}^2}{2}, \qquad r = \frac{m_{\tilde{t}_L}^2 - m_{\tilde{t}_R}^2}{m_{\tilde{t}_L}^2 + m_{\tilde{t}_R}^2}, \tag{2.16}$$

then the cross section $\sigma(gg \to h)$ only depends on $m_{\tilde{t}}^2$ and X_t mostly; the dependence on r is minimal when $|r| \lesssim 0.4$. In figure 1 we show that this is the case also in the ratio of the event rate $B\sigma(gg \to h \to \gamma\gamma)$ as well. From the figure we see that the variation in the ratio of $B\sigma(gg \to h \to \gamma\gamma)$ is less than 10% for large X_t if $r \lesssim 0.5$. For $m_{\tilde{t}} = 500\,\text{GeV}$ this translates into $m_{\tilde{t}_L} \sim 600\,\text{GeV}$ and $m_{\tilde{t}_R} \sim 300\,\text{GeV}$.

It turns out that, as pointed out in Ref . [5], the Higgs mass m_h is also sensitive to the same two parameters in the stop mass matrix. Thus in the end two measurements in m_h and $B\sigma$ could potentially yield useful information on two mass parameters, including X_t, in the stop sector of the MSSM.

3 The Higgs mass in the MSSM

In this section we very briefly discuss the mass of the lightest CP-even Higgs in the MSSM, as much of it has been studied extensively in the literature. The Higgs sector of the MSSM contains two Higgs doublets, H_u and H_d, which couples to the up-type and down-type quarks separately due to constraints from the anomaly cancellation and the holomorphicity of the superpotential. After electroweak symmetry breaking five remaining physical

states are two CP-even neutral Higgs bosons, h (the lighter one) and H (the heavier one), one CP-odd neutral Higgs boson A, and the charged Higgses $H^{\pm}$. In the MSSM there are two free parameters in the Higgs sector, taken to be $\tan\beta$ and m_A, and at tree level one can derive an upper bound on m_h [10]:

$$m_h \leq m_Z |\cos 2\beta| \leq m_Z = 91.2 \text{ GeV}, \tag{3.1}$$

which is well below the direct search limit of 114 GeV at LEP.

Therefore, large radiative corrections from superparticles with significant couplings to h are required to raise m_h above the LEP bound. Among the new particles in MSSM the stops have the largest coupling to the lightest CP-even Higgs due to the top Yukawa couplings. (We are avoiding the region of very large $\tan\beta$ and large μ where the sbottom couplings could also be significant, as mentioned in the previous section.) If we assume for simplicity $m_{\tilde{t}_R} \simeq m_{\tilde{t}_L} = m_{\tilde{t}}$, the one-loop correction to m_h is approximately given as [10, 23]

$$\Delta m_h^2 \simeq \frac{3 G_F}{\sqrt{2}\pi^2} m_t^4 \left\{ \log \frac{m_{\tilde{t}}^2}{m_t^2} + \frac{X_t^2}{m_{\tilde{t}}^2} \left(1 - \frac{X_t^2}{12 m_{\tilde{t}}^2} \right) \right\}, \tag{3.2}$$

which grows only logarithmically with the stop mass $m_{\tilde{t}}$. Therefore to lift m_h from m_Z to be above 114 GeV requires very heavy stops if there is no large mixing. Typically for $m_{\tilde{t}_R} \simeq m_{\tilde{t}_L}$ the stop masses need to be very large, $\mathcal{O}(1\,\text{TeV})$, to evade the LEP bound. On the other hand, the up-type Higgs mass-squared increases quadratically with $m_{\tilde{t}}$,

$$\Delta m_{H_u}^2 \simeq -\frac{3}{8\pi^2} m_{\tilde{t}}^2 \log \frac{\Lambda^2}{m_{\tilde{t}}^2}. \tag{3.3}$$

Thus heavy stop masses at around 1 TeV would lead to large ($\mathcal{O}(m_Z^2/m_{\tilde{t}}^2) \lesssim 1\%$) fine-tuning in electroweak symmetry breaking. However, the fine-tuning can be reduced if the stop masses could be significantly below 1 TeV while at the same time keeping $m_h \gtrsim 114$ GeV. This is possible only if there is large mixing in the stop sector, in which case the fine tuning can be reduced to the level of 5%. The Higgs mass is maximized for $|X_t/m_{\tilde{t}}| \sim 2$ and with this mixing light stops, $m_{\tilde{t}_R} \simeq m_{\tilde{t}_L} \simeq 300$ GeV, are sufficient to raise the Higgs mass above the LEP limit.

4 Results

We use the program `FeynHiggs-2.6.4` [24, 25] in our numerical analysis with the following relevant parameters: $m_t = 172.6$ GeV, $m_b = 4.2$ GeV, and the pseudo-scalar Higgs mass $m_A = 400$ GeV (unless otherwise noted.) It is perhaps worth emphasizing that `FeynHiggs` employs various approximation schemes in computing the MSSM Higgs production and decay rates, which are extrapolated from the SM predictions. In this work we use the program mainly to study the dependence on other SUSY parameters and demonstrate the feasibility of our proposal. Higher-order QCD corrections could be important and should be included if a full-fledged analysis were performed, which is beyond the scope of the current work. In the following the main observable we consider is the ratio of the event
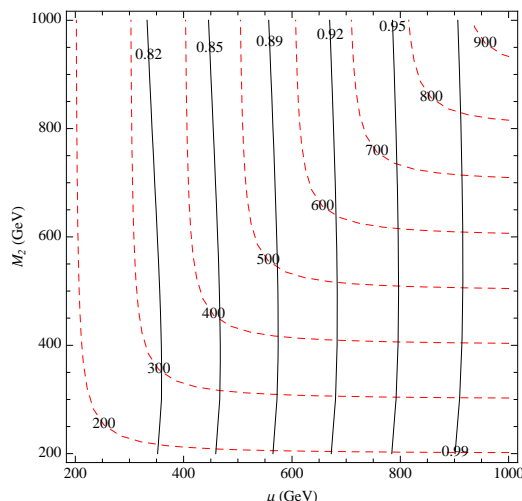
Figure 2. Contour plot of m_{χ_1} and $R(B\sigma)$ in the $\mu - M_2$ plane. In this plot $\tan\beta = 30$, $M_{\text{SUSY}} = 1000\,\text{GeV}$, $m_{\tilde{t}_L} = m_{\tilde{t}_R} = 500\,\text{GeV}$, and $X_t = -700\,\text{GeV}$. The (dark) solid lines correspond to the $R(B\sigma)$ contours, whereas the (red) dashed lines are for the m_{χ_1} contours. This set of parameters would result in a Higgs mass slightly above the LEP bound of $114\,\text{GeV}$.

rates in the MSSM over the standard model: $R(B\sigma) = B\sigma(\text{MSSM})/B\sigma(\text{SM})$. (When we speak of the event rate, we would always have in mind the ratio of the event rates!)

We first consider the effect of the chargino mass on $R(B\sigma)$. In MSSM the chargino mass is determined by the gaugino mass parameter M_2 and the supersymmetric Higgs mass parameter μ. In figure 2 we present a contour plot of $R(B\sigma)$ and the lightest chargino mass m_{χ_1} in the $\mu - M_2$ plane, in which m_{χ_1} varies from 200 to $900\,\text{GeV}$. We see that contours of constant $R(B\sigma)$ runs somewhat parallel to the M_2 axis, which implies $R(B\sigma)$ is sensitive to μ only. Therefore $R(B\sigma)$ depends on the chargino mass only through its dependence on the μ parameter. For example, let's choose $\mu = 900\,\text{GeV}$ and change M_2 from 200 to $1000\,\text{GeV}$, which results a modification in m_{χ_1} from 200 to $900\,\text{GeV}$. The corresponding $R(B\sigma)$ remains roughly constant at 0.99, as can be seen from figure 2, in spite of a large variation in m_{χ_1}. On the other hand, one could vary μ while keeping m_{χ_1} constant, and $R(B\sigma)$ would change significantly according to μ. It has been previously observed that the chargino has a small effect in the partial width $\Gamma(h \to \gamma\gamma)$ [12]. Here we see what is important is the value of the μ parameter, instead of the chargino mass itself. If μ is not too large, then the effect of the chargino is small not only in the partial width of $h \to \gamma\gamma$, but also in the ratio of the event rate $B\sigma(gg \to h \to \gamma\gamma) = \sigma(gg \to h) \times Br(h \to \gamma\gamma)$.

On the other hand, we observe in figure 2 that $R(B\sigma)$ does have a strong dependence in the supersymmetric Higgs mass parameter μ. From the discussion above we know this dependence cannot come from the charginos. It turns out the μ dependence does not arise from effects of supersymmetric particles in either the production cross-section $\sigma(gg \to h)$ or the partial decay width $\Gamma(h \to \gamma\gamma)$. Somewhat surprisingly, the strong μ dependence resides in the radiative corrections of supersymmetric particles to the bottom Yukawa coupling. The bottom Yukawa coupling controls the decay amplitude of $h \to b\bar{b}$, which partial width dominates the total decay width of the lightest CP-even Higgs in MSSM.
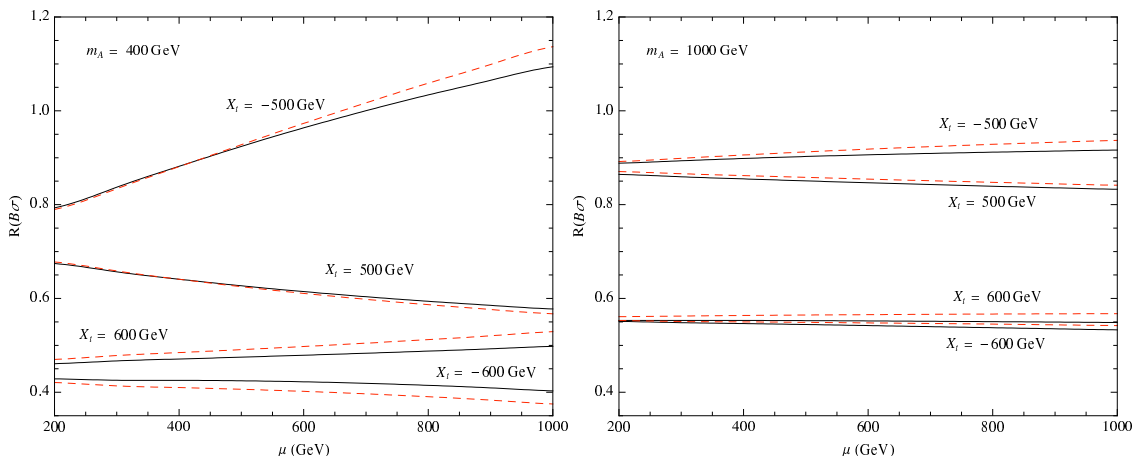
Figure 3. Dependence on μ in the event rate $R(B\sigma)$. In these plots $\tan\beta = 30$, $M_{\rm SUSY} = 500$ (solid lines) and 1000 (dashed lines) GeV, $m_{\tilde{t}_L} = m_{\tilde{t}_R} = 300\,{\rm GeV}$, and $X_t = \pm 500$ and $\pm 600\,{\rm GeV}$. The two choices of X_t correspond a Higgs mass of 116 and 119 GeV, respectively. The left plot is for $m_A = 400\,{\rm GeV}$ and the right for $m_A = 1000\,{\rm GeV}$. In the plots we have also set the gaugino mass parameter $M_2 = M_{\rm SUSY}$.

Since the branching ratio is given as

$$Br(h \to \gamma\gamma) = \frac{\Gamma(h \to \gamma\gamma)}{\Gamma_{\rm tot}} \approx \frac{\Gamma(h \to \gamma\gamma)}{\Gamma(h \to b\bar{b})}, \qquad (4.1)$$

the event rate $B\sigma$ is very sensitive to supersymmetric corrections to $h \to b\bar{b}$.

More specifically, at one-loop the running b-quark mass receives contributions from sbottom-gluino loops and stop-charged Higgsino loops,[2] [26–28] which depends on the gluino mass, the stop and sbottom eigenmasses, the supersymmetric Higgs mass μ as well as the stop mixing parameter X_t. Such corrections become more important when $\tan\beta$ becomes larger, which is the regime we are interested in. However, since we are avoiding regions where the sbottoms are light, we find the sbottom-gaugino loop is numerically unimportant. In figure 3 we single out the μ dependence of $R(B\sigma)$ for $\tan\beta = 30$ and some choices of stop masses and X_t. The reason that the variation is asymmetric in $X_t \to -X_t$ is because the contribution from stop-chargino loop is linear in X_t at leading order. So for one sign it adds to the tree-level result while for the opposite sign it subtracts. Nevertheless, the important observation is that as the mixing parameter X_t becomes larger, the variation becomes smaller. In this case, one of the stop mass eigenstates is heavy and suppresses the loop contributions. Therefore if we are only interested in the MSSM golden region, where X_t is large and $|X_t/m_{\tilde{t}}| \sim 2$, the μ dependence is reduced.

The fact that the total decay width $\Gamma_{\rm tot} \approx \Gamma(h \to b\bar{b})$ enters into $Br(gg \to h \to \gamma\gamma)$ introduces additional sensitivity on the mass of the pseudo-scalar Higgs m_A, which is absent in either the cross-section $\sigma(gg \to h)$ or the partial decay width $\Gamma(h \to \gamma\gamma)$, because the Higgs coupling to bottom quarks depends on m_A in a complicated fashion. When normal-

---

[2]There is also a sbottom-wino loop whose contribution is suppressed by the smallness of the electroweak gauge coupling.
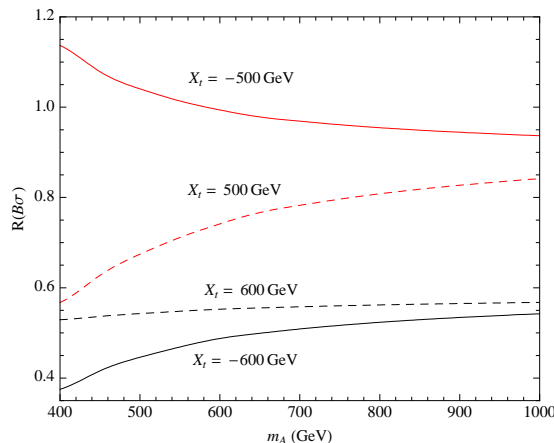
Figure 4. Dependence of $R(B\sigma)$ on m_A. In this plot $\tan\beta = 30$, $M_{\text{SUSY}} = 1000\,\text{GeV}$, $m_{\tilde{t}_L} = m_{\tilde{t}_R} = 300\,\text{GeV}$, and $X_t = \pm 500$ and $\pm 600\,\text{GeV}$. These two choices of X_t correspond a Higgs mass of 116 and 119 GeV, respectively. In the plot we have set $\mu = M_2 = M_{\text{SUSY}}$.

izing to im_b/v, the tree-level Higgs coupling to bottom quarks in MSSM can be written as

$$g_{hbb} = -\frac{\sin\alpha}{\cos\beta}; \qquad \alpha = \frac{1}{2}\arctan\left(\tan 2\beta\frac{m_A^2 + m_Z^2}{m_A^2 - m_Z^2}\right), \qquad (4.2)$$

where α is the mixing angle in the CP-even Higgs sector and $-\pi/2 \leq \alpha \leq 0$. The usual decoupling regime of MSSM, where the lightest CP-even Higgs has standard model-like couplings, is obtained in the limit of large $\tan\beta$ and $m_A \gg m_Z$. In this limit the Higgs coupling to the standard model gauge bosons, $g_{hVV} \propto \sin(\beta - \alpha) \to 1$, approaches that of a standard model Higgs boson. This limit happens quite fast for moderately heavy m_A and one some times define the decoupling regime as the region where $\sin^2(\beta - \alpha) \geq 0.95$ [10]. However, because the Higgs coupling to bottom quarks is proportional to $-\sin\alpha/\cos\beta$, instead of $\sin(\beta - \alpha)$, g_{hbb} approaches its standard model value much slower than the g_{hVV} couplings. For example, at $\tan\beta = 30$ and $m_A = 400\,\text{GeV}$, we have $\sin^2(\beta - \alpha) = 0.99999$ whereas g_{hbb}^2 is only 0.81, still quite far from the standard model value at unity. In figure 4 we plot the m_A dependence of the event rate $R(B\sigma)$ and one sees that the sensitivity is quite strong in varying m_A from 400 to 1000 GeV, especially for a light Higgs mass $m_h \approx 116\,\text{GeV}$.

The slow approach to the decoupling limit of the tree-level coupling in g_{hbb} is indicative of the strong m_A dependence in $\Gamma(h \to b\bar{b})$, and hence Γ_{tot}. However, the sensitivity in figure 4 cannot be explained by the change in the tree-level coupling alone, and higher-order corrections play an important role here. Since m_A is taken as one of the input parameters in the Higgs sector of MSSM, it is clear that m_A enters into the higher-order corrections in a complicated way and its effect cannot be disentangled easily. For example, in addition to the supersymmetric loop corrections to the bottom Yukawa couplings mentioned previously, there are also higher-order corrections to the off-diagonal matrix element of the CP-even Higgs mass matrix [29, 30]. We would perhaps only comment that all these higher-order corrections have been incorporated in the numerical code `FeynHiggs` [31], which is employed in this study. It is also worth observing that the dependence of $R(B\sigma)$ on μ becomes weaker for large pseudo-scalar mass m_A, as can be seen in figure 3.
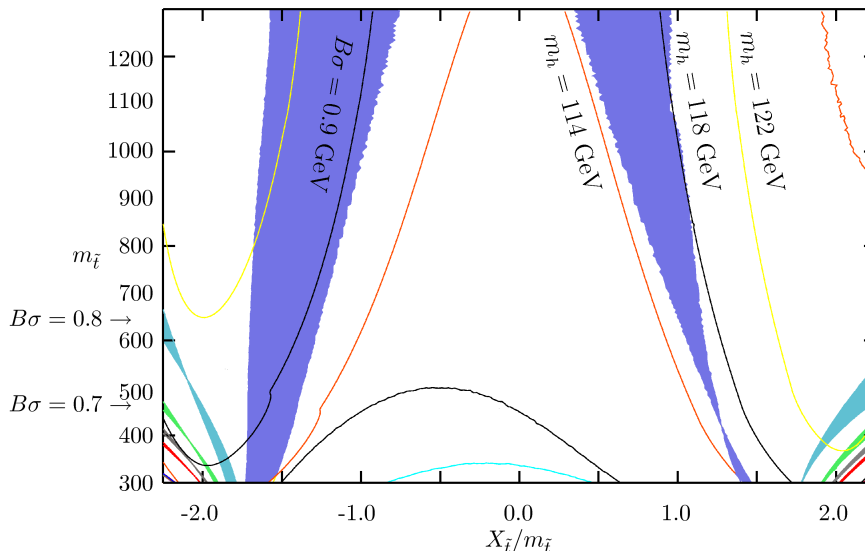
Figure 5. Contours of $R(B\sigma)$ and m_h in the $m_{\tilde{t}} - X_t/m_{\tilde{t}}$ plane. This plot is for $\tan\beta = 30$, $M_{\text{SUSY}} = 1000\,\text{GeV}$, and $m_A=1000\,\text{GeV}$. The shaded regions correspond to the variation in $R(B\sigma)$ when changing μ from 200 to 1000 GeV.

Given the strong m_A dependence and, to a less extent, the μ dependence in $R(B\sigma)$, it is desirable to have knowledge of these two input parameters before one can use both m_h and $B\sigma$ to extract $m_{\tilde{t}}$ and X_t in the stop sector. This is contrary to the case of utilizing the the Higgs production rate in the gluon fusion channel in conjuction with m_h, as suggested in [5], where the sensitivity to SUSY parameters other than $m_{\tilde{t}}$ and X_t are very weak. In figure 5 we present contours of $R(B\sigma)$ and m_h in the $m_{\tilde{t}} - X_t/m_{\tilde{t}}$ plane for $m_A = 1000\,\text{GeV}$. In the plot we have included the μ dependence by varying μ from 200 to 1000 GeV and using the shaded region to represent the corresponding change in $R(B\sigma)$. We see that in the region where X_t is small and the MSSM fine-tuned, the $R(B\sigma)$ contour runs somewhat parallel to the m_h contours and no useful information on $m_{\tilde{t}}$ and X_t could be extracted. On the other hand, in the less fine-tuned MSSM golden region where the stops are light and X_t is large, the two contours run almost perpendicular to each other and one could potentially get a fair estimate on the magnitudes of $m_{\tilde{t}}$ and X_t. Moreover, in this region of particular interests, $R(B\sigma)$ deviates substantially from unity in that the event rate in the MSSM is much smaller than in the standard model, which implies it may take longer time and more statistics to observe the Higgs at the LHC if indeed the MSSM is realized in nature in a less fine-tuned region of parameter space. In addition, the variation due to μ in $R(B\sigma)$ is also smaller in this particular region.

In figure 6 we focus in the region where $300\,\text{GeV} \leq m_{\tilde{t}} \leq 600\,\text{GeV}$ and $-2.25 \leq X_t/m_{\tilde{t}} \leq -1.0$ for two different values of m_A at 400 and 1000 GeV. We have chosen the minus sign for X_t since constraints from rare B decays seem to favor negative X_t [32]. As commented previously, the variation due to μ is larger for smaller value of m_A. We see that it is important to know the mass of the pseudo-scalar Higgs m_A. But once m_A is known, one could get a fair estimate of $m_{\tilde{t}}$ and X_t even without prior knowledge of the supersymmetric Higgs mass μ, especially in the region where $R(B\sigma) \lesssim 0.8$.

– 10 –
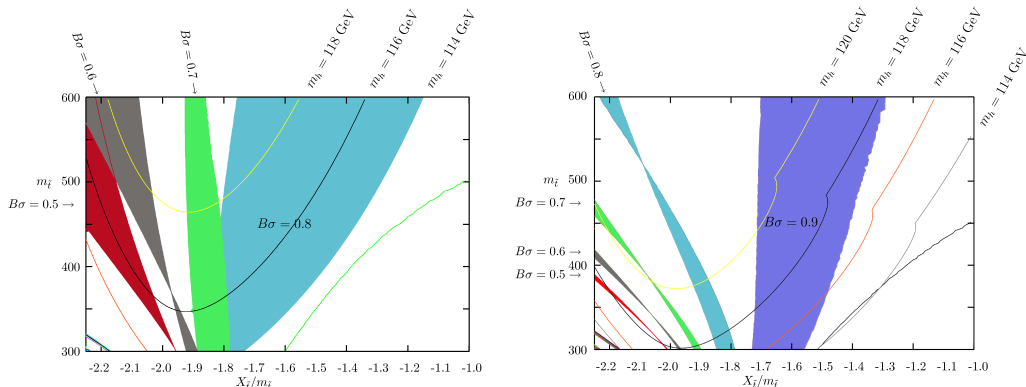
Figure 6. Contours of $R(B\sigma)$ and m_h in the MSSM golden region. In these plots $\tan\beta = 30$ and $M_{\text{SUSY}} = 1000\,\text{GeV}$. In the top plot $m_A = 400\,\text{GeV}$ and in the bottom plot $m_A = 1000\,\text{GeV}$. The shaded regions have the same meaning as in figure 5.

5 Conclusion

In this work we studied implications of discovering the lightest CP-even Higgs boson in the MSSM golden region, when measurements on the Higgs mass m_h and the event rate $B\sigma(gg \to h \to \gamma\gamma)$ are made at the same time. Previously it was suggested that m_h and the Higgs production cross-section in the gluon fusion channel could be used to extract two parameters, $m_{\tilde{t}}$ and X_t, in the stop sectors, which are important to understand the degree of fine-tuning in the MSSM. We find that in the case of the event rate there are additional sensitivities on the pseudo-scalar mass m_A and the supersymmetric Higgs mass μ. It turns out that both sensitivities result from the Higgs coupling to bottom quarks, which partial decay width dominates the total decay width of the lightest CP-even Higgs boson in the MSSM. The fact that the branching ratio $Br(h \to \gamma\gamma)$ depends on the total width introduces sizable dependence of $B\sigma$ on m_A and μ, even though neither the production cross-section $\sigma(gg \to h)$ nor the partial decay width $\Gamma(h \to \gamma\gamma)$ is sensitive to these two parameters. We also find that, in the MSSM golden region where the stops are light and the mixing is large, the most important input parameter is m_A, whereas ignorance of μ could still allow for a fair estimate of $m_{\tilde{t}}$ and X_t in the stop sector. Moreover, we find that throughout the MSSM golden region the event rate $B\sigma$ is significantly smaller than the standard model rate, which implies it may take more time to make the discovery. Given that there is no known method to directly measure the stop mixing parameter X_t, it will be important to combine the study presented here with the proposal in ref. [5] to get indirect measurements on $m_{\tilde{t}}$ and X_t.

Acknowledgments

References

[1] R. Kitano and Y. Nomura, *A solution to the supersymmetric fine-tuning problem within the MSSM*, *Phys. Lett.* **B 631** (2005) 58 [hep-ph/0509039] [SPIRES].

[2] G.F. Giudice and R. Rattazzi, *Living dangerously with low-energy supersymmetry*, *Nucl. Phys.* **B 757** (2006) 19 [hep-ph/0606105] [SPIRES].

[3] M. Perelstein and C. Spethmann, *A collider signature of the supersymmetric golden region*, *JHEP* **04** (2007) 070 [hep-ph/0702038] [SPIRES].

[4] R. Kitano and Y. Nomura, *Supersymmetry, naturalness and signatures at the LHC*, *Phys. Rev.* **D 73** (2006) 095004 [hep-ph/0602096] [SPIRES].

[5] R. Dermisek and I. Low, *Probing the stop sector and the sanity of the MSSM with the Higgs boson at the LHC*, *Phys. Rev.* **D 77** (2008) 035012 [hep-ph/0701235] [SPIRES].

[6] R. Essig, *Implications of the LEP Higgs bounds for the MSSM stop sector*, *Phys. Rev.* **D 75** (2007) 095005 [hep-ph/0702104] [SPIRES].

[7] R. Essig and J.-F. Fortin, *The minimally tuned minimal supersymmetric standard model*, *JHEP* **04** (2008) 073 [arXiv:0709.0980] [SPIRES].

[8] J. Kasahara, K. Freese and P. Gondolo, *Dark matter in the MSSM golden region*, *Phys. Rev.* **D 79** (2009) 045020 [arXiv:0805.0999] [SPIRES].

[9] W.S. Cho, Y.G. Kim and C.B. Park, *Comment on 'A collider signature of the supersymmetric golden region'*, *JHEP* **12** (2008) 074 [arXiv:0809.0043] [SPIRES].

[10] A. Djouadi, *The anatomy of electro-weak symmetry breaking. II. The Higgs bosons in the minimal supersymmetric model*, *Phys. Rept.* **459** (2008) 1 [hep-ph/0503173] [SPIRES].

[11] For a comprehensive review, see A. Djouadi, *The anatomy of electro-weak symmetry breaking. I: the Higgs boson in the standard model*, *Phys. Rept.* **457** (2008) 1 [hep-ph/0503172] [SPIRES].

[12] A. Djouadi, V. Driesen, W. Hollik and J.I. Illana, *The coupling of the lightest SUSY Higgs boson to two photons in the decoupling regime*, *Eur. Phys. J.* **C 1** (1998) 149 [hep-ph/9612362] [SPIRES].

[13] A. Djouadi, *Squark effects on Higgs boson production and decay at the LHC*, *Phys. Lett.* **B 435** (1998) 101 [hep-ph/9806315] [SPIRES].

[14] M. Dührssen et al., *Extracting Higgs boson couplings from LHC data*, *Phys. Rev.* **D 70** (2004) 113009 [hep-ph/0406323] [SPIRES].

[15] C. Anastasiou, K. Melnikov and F. Petriello, *The gluon-fusion uncertainty in Higgs coupling extractions*, *Phys. Rev.* **D 72** (2005) 097302 [hep-ph/0509014] [SPIRES].

[16] H.E. Haber, *Challenges for nonminimal Higgs searches at future colliders*, hep-ph/9505240 [SPIRES].

[17] J.R. Ellis, M.K. Gaillard and D.V. Nanopoulos, *A phenomenological profile of the Higgs boson*, *Nucl. Phys.* **B 106** (1976) 292 [SPIRES].

[18] H.M. Georgi, S.L. Glashow, M.E. Machacek and D.V. Nanopoulos, *Higgs bosons from two gluon annihilation in proton proton collisions*, *Phys. Rev. Lett.* **40** (1978) 692 [SPIRES].

[19] M.A. Shifman, A.I. Vainshtein, M.B. Voloshin and V.I. Zakharov, *Low-energy theorems for Higgs boson couplings to photons*, *Sov. J. Nucl. Phys.* **30** (1979) 711 [*Yad. Fiz.* **30** (1979) 1368] [SPIRES].

[20] J.F. Gunion, H.E. Haber, G.L. Kane and S. Dawson, *The Higgs hunter's guide*, Addison-Wesley (1990) [SPIRES].

[21] PARTICLE DATA GROUP collaboration, W.M. Yao et al., *Review of particle physics*, *J. Phys.* **G 33** (2006) 1 [SPIRES].

[22] A. Brignole, G. Degrassi, P. Slavich and F. Zwirner, *On the two-loop sbottom corrections to the neutral Higgs boson masses in the MSSM*, *Nucl. Phys.* **B 643** (2002) 79 [hep-ph/0206101] [SPIRES].

[23] H.E. Haber, R. Hempfling and A.H. Hoang, *Approximating the radiatively corrected Higgs mass in the minimal supersymmetric model*, *Z. Phys.* **C 75** (1997) 539 [hep-ph/9609331] [SPIRES].

[24] S. Heinemeyer, W. Hollik and G. Weiglein, *FeynHiggs: a program for the calculation of the masses of the neutral CP-even Higgs bosons in the MSSM*, *Comput. Phys. Commun.* **124** (2000) 76 [hep-ph/9812320] [SPIRES].

[25] M. Frank et al., *The Higgs boson masses and mixings of the complex MSSM in the Feynman-diagrammatic approach*, *JHEP* **02** (2007) 047 [hep-ph/0611326] [SPIRES].

[26] L.J. Hall, R. Rattazzi and U. Sarid, *The top quark mass in supersymmetric* SO(10) *unification*, *Phys. Rev.* **D 50** (1994) 7048 [hep-ph/9306309] [SPIRES].

[27] R. Hempfling, *Yukawa coupling unification with supersymmetric threshold corrections*, *Phys. Rev.* **D 49** (1994) 6168 [SPIRES].

[28] M.S. Carena, M. Olechowski, S. Pokorski and C.E.M. Wagner, *Electroweak symmetry breaking and bottom-top Yukawa unification*, *Nucl. Phys.* **B 426** (1994) 269 [hep-ph/9402253] [SPIRES].

[29] M.S. Carena, S. Mrenna and C.E.M. Wagner, *MSSM Higgs boson phenomenology at the Tevatron collider*, *Phys. Rev.* **D 60** (1999) 075010 [hep-ph/9808312] [SPIRES].

[30] S. Heinemeyer, W. Hollik and G. Weiglein, *Decay widths of the neutral CP-even MSSM Higgs bosons in the Feynman-diagrammatic approach*, *Eur. Phys. J.* **C 16** (2000) 139 [hep-ph/0003022] [SPIRES].

[31] T. Hahn, S. Heinemeyer, W. Hollik, H. Rzehak and G. Weiglein, *Higgs masses and more in the complex MSSM with FeynHiggs*, in the Proceedings of the *15th International conference on supersymmetry and the unification of fundamental interactions (SUSY07)*, Karlsruhe, Germany, July 26 – August 1 2007, arXiv:0710.4891 [SPIRES].

[32] M. Carena, A. Menon and C.E.M. Wagner, *Minimal flavor violation and the scale of supersymmetry breaking*, arXiv:0812.3594 [SPIRES].